Ondrej Zitka[1,2]
Zbynek Heger[1]
Marketa Kominkova[1]
Sylvie Skalickova[1]
Sona Krizkova[1,2]
Vojtech Adam[1,2]
Rene Kizek[1,2]

[1]Department of Chemistry and Biochemistry, Faculty of Agronomy, Mendel University in Brno, Brno, Czech Republic
[2]Central European Institute of Technology, Brno University of Technology, Brno, Czech Republic

Received November 6, 2013
Revised December 16, 2013
Accepted December 18, 2013

Research Article

Preconcentration based on paramagnetic microparticles for the separation of sarcosine using hydrophilic interaction liquid chromatography coupled with coulometric detection

Sarcosine has been identified as a potential prostate cancer marker. To provide determination of this compound, a number of methods are developing. In this study, we optimized a method for its separation by hydrophilic interaction LC with electrochemical detection (ED). Due to the fact that mobile phases commonly used for this type of separation altered the LODs measured by electrochemical detectors, we applied postcolumn dosing of buffer suitable for ED. The optimized conditions were mobile phase A acetonitrile, mobile phase B water in the ratio A/B 70:30, with postcolumn addition of mobile phase C (200 mM phosphate buffer pH 9). The optimal mixing ratio was A + B/C 1:1 with a flow rate of 0.80 mL/min (0.40 + 0.40 mL/min) and detection potential of 1000 mV. Due to the optimization of the parameters for effective separation, which had to meet the optimal parameters of ED, we reached a good resolution for separation also with a good LOD (100 nM). In addition, we successfully carried out sarcosine analysis bound on our modified paramagnetic microparticles with the ability to preconcentrate sarcosine isolated from artificial urine.

Keywords: Paramagnetic separation / Prostate cancer / Sarcosine / Urinary metabolites
DOI 10.1002/jssc.201301188

1 Introduction

Sarcosine, chemically defined as the methyl derivative of glycine, formed in the mammalian body as an intermediate product of choline, methionine, glycine, creatine, purine, and serine metabolic cycles, was first isolated and characterized by German chemist Justus von Liebig in 1847 [1]. In 2009, sarcosine was highlighted as a potential cancer marker able to distinguish benign, localized, and metastatic prostate tumors, but the most attractive was the possibility to detect this molecule not only from blood but also from urine, which could open a window for simple and noninvasive diagnostics [2]. However, the opinions on sarcosine application in this area are inconsistent and publications refuting its applicability as a tumor disease marker have appeared [3–7]. To verify the hypothesis of the marker new methods for robust and accurate sarcosine determination have to be found.

Commercial kits, based on its specific oxidation yielding a product that convert a colorless probe to a product with intense red color (max = 570 nm) and which is also highly fluorescent (Ex/Em = 538/587 nm) are mostly utilized for sarcosine detection. The detection limit of this method is estimated as 1 μM (Abcam's Sarcosine Assay Kit, BioVision Sarcosine Assay Kit) by the manufacturer. In a study by Burton et al., sarcosine was analyzed using the fluorescence detection of formaldehyde resulting as a product of an enzymatic cleaving of sarcosine with a LOD down to 20 nM [8]. Sarcosine, as well as other amino acids can be analyzed by IEC with UV or fluorescent detection [9] or by RP HPLC with UV, electrochemical [10] and fluorescent detection [11], but the spectral detection methods still require sample preparation, mostly on solid phase, with subsequent derivatization [2, 12–14]. For sarcosine determination, LC–MS can be used, which however exhibits lower distinguishability of sarcosine from its isomer alanine [3, 15]. Possible coelution of these substances could be resolved by utilization of tandem differential mobility analysis with MS [16]. Besides LC, mass detection linked with GC provides also sensitivity and high reproducibility in the case of sarcosine detection [6]. CE was also shown as a possible method in this field of interest [17].

Hydrophilic interaction chromatography (HILIC) was developed in 1990s [18]. HILIC is suitable for hydrophilic and polar compounds both macromolecular (such as histones and membrane proteins) as well as low-molecular-weight compounds (such as phosphorylated amino acids and peptides) [19, 20]. HILIC columns excel in high efficiency and

Correspondence: Dr. Rene Kizek, Department of Chemistry and Biochemistry, Mendel University in Brno, Zemedelska 1, CZ-613 00 Brno, Czech Republic
E-mail: kizek@sci.muni.cz
Fax: +420-5-4521-2044

Abbreviations: **ACN**, acetonitrile; **DAD**, diode array detector; **ED**, electrochemical detection; **ESI-Q-TOF-MS**, ESI quadrupole TOF-MS; **HILIC**, hydrophilic interaction chromatography; **PMP**, paramagnetic microparticle; **SECM**, scanning electrochemical microscope

Colour Online: See the article online to view Figs. 1–6 in colour.

short analysis time. The low viscosity of mobile phases ensures high analytical performance, which can be achieved only by using high separation temperatures at reverse phases. Inferior solubility in mobile phases can be considered as a disadvantage for some analytes. MS [21,22], UV detection [23,24], fluorescence detection, or diode array detection [25] are the most common ways of detection utilized in connection with hydrophobic chromatography. Rarely, electrochemical detection (ED) can be also used due to an inappropriate nature of polar mobile phases used at HILIC analysis [26].

The aim of this study was to develop a method for the detection of low concentrations of sarcosine and to utilize the advantages of HILIC and the compactness of coulometric detection. An additional objective was the verification of the usefulness of our modified paramagnetic microparticles (PMPs) that may be used for sarcosine preconcentration in urine samples containing low amounts of this amino acid.

2 Material and methods

2.1 Chemicals

Sarcosine, acetonitrile (ACN), Na_2HPO_4, NaH_2PO_4, and others were purchased from Sigma-Aldrich (St. Louis, MO, USA) in ACS purity, unless noted otherwise. Working solutions as buffers or standard solution of sarcosine were prepared daily by diluting the stock solutions. The deionized water was further purified by using MilliQ Direct QUV apparatus equipped with a UV lamp. The resistance was 18 MΩ. The pH was measured by using a pH meter WTW inoLab (Weilheim, Germany).

2.2 Preparation of PMPs

PMPs were prepared by sodium borohydride ($NaBH_4$) reduction of iron chloride ($FeCl_3.6H_2O$). Briefly, 10 g of $FeCl_3{\cdot}6H_2O$ was dissolved in 800 mL of MilliQ water and a solution of 2 g of $NaBH_4$ in ammonia (3.5%, 100 mL, *m/v*) was poured into the first solution with vigorous stirring. The obtained solution was heated at 100°C for 2 h. After cooling the obtained magnetic nanoparticles were separated by external magnetic field and washed five times with water. Thus prepared nanoparticles were suspended in 80 mL of water and 5 mL of tris(perchlorate)gadolinium ($Gd(ClO_4)_3$). The mixture was shaken for 12 h at room temperature and after that separated by external magnetic field and washed several times with water. Product was dried at 40°C. Thus prepared PMPs were ready for further analyses.

2.3 SEM characterization

Structure of PMPs was characterized by SEM. For documentation of the PMPs structure a MIRA3 LMU (Tescan, Brno, Czech Republic) was used. This model is equipped with a high brightness Schottky field emitter for low noise imaging at fast scanning rates. The SEM was fitted with In-Beam SE detector. Samples were coated by 5 nm of platinum to prevent sample charging. For automated acquisition of selected areas a TESCAN proprietary software tool called Image Snapper was used. The software enables automatic acquisition of selected areas with defined resolution. An accelerating voltage of 15 kV and beam currents about 1 nA gives satisfactory results regarding maximum throughput.

2.4 Scanning electrochemical microscopic characterization of PMPs after interaction with sarcosine

We carried out the identification of relative current response before and after sarcosine binding to PMPs obtained by scanning electrochemical microscope Model 920D (CH instruments, Austin, TX, USA). The electrochemical microscope consisted of a 10 mm platinum disc probe electrode with potential of 0.2 V. Another platinum disc electrode with an O-ring as the conducting substrate used potential of 0.3 V. During scanning, the particles were attached on the substrate platinum electrode by magnetic force from neodymium magnet, situated below the electrode. The platinum-measuring electrode moved at least 150 μm above the surface. The solvent mixture for analysis of PMPs consisted of 5% ferrocene in methanol mixed in ratio 1:1 with 0.05% KCl in water v/v. The measurement was performed in Teflon cell with volume of 1.5 mL under the following parameters: amperometric mode, vertical scan was carried out in the area 500 × 500 μm with a rate of 30 μm/s.

2.5 X-ray fluorescence analysis of PMPs

X-ray fluorescence elemental analysis of the PMPs was carried out on Xepos (SPECTRO Analytical Instruments, Kleve, Germany) fitted with three detectors: Barkla scatter-aluminium oxide, Barkla scatter-HOPG and Compton/secondary molybdenum detector, respectively. Analyses were conducted according to the Turbo Quant cuvette method of measuring. Analysis parameters were set to as follows: measurement duration: 300 s, tube voltage from 24.81 to 47.72 kV, tube current from 0.55 to 1.0 mA, with zero peak at 5000 cps and vacuum switched off.

2.6 Preparation of samples for analysis using PMPs

PMPs able to isolate and immobilize sarcosine were prepared in stock solution, which consisted of 40 mg PMPs in 1000 μL of PBS. The stock solution was subsequently treated with ultrasonic homogenizer SONOPULS mini20 (Bandelin electronic, Berlin, Germany) for 2 min. Such diluted 50 μL of PMPs were mixed together with 200 μL of PBS prior to further experiments. Particles were washed three times with PBS and three times with Britton–Robinson buffer with

pH 2 using a permanent magnet (Chemagen, Baesweiler, Germany) for removing undesirable impurities. Then a binding between sarcosine and PMPs was established in conformity of optimized conditions according to Zitka et al. [27]. Then another three washing steps with Britton–Robinson buffer were applied. Remaining retentate consisting of PMPs with sarcosine was dissolved in 3 M HCl and shaken for 10 min with 1250 rpm in thermoblock Thermomixer® R (Eppendorf, Hamburg, Germany) for better particles dissolution. Dissolved PMPs were transferred into 96-well evaporation plate (Deepwell plate 96, Eppendorf AG, Hamburg, Germany) and evaporated. For evaporation of dissolved PMPs the nitrogen blow-down evaporator Ultravap 96 with spiral needles (Porvair Sciences, Leatherhead, UK) was used. Evaporated sample was resuspended with dilution buffer instead of ESI quadrupole TOF MS (ESI-Q-TOF-MS) analysis, where isopropanol was used for resuspension and subsequent dilution. A sample prepared in this way was ready for analyses using ion exchange LC with UV detection, ESI-Q-TOF-MS, and HILIC with ED.

2.7 Ion exchange LC

For confirmation of sarcosine presence on our PMPs an ion exchange LC (Model AAA-400, Ingos, Prague, Czech Republic) with postcolumn derivatization by ninhydrin and absorbance detection in the visible light range (VIS) was used. A glass column with an inner diameter of 3.7 mm and 350 mm length was filled manually with strong cation exchanger in sodium cycle LG ANB with approximately 12 μm particles and 8% porosity. The column was tempered at 60°C. Double channel VIS detector with inner cell of 5 μL volume was set to two wavelengths: 440 and 570 nm. A solution of ninhydrin (Ingos) was prepared in 75% methylcelosolve (v/v, Ingos) and in 2% v/v 4 M acetate buffer (pH 5.5). Tin chloride ($SnCl_2$) was used as a reducing agent. The prepared solution of ninhydrin was stored under inert atmosphere (N_2) in the dark at 4°C. The elution of sarcosine was done by a buffer containing 10.0 g of citric acid, 5.6 g of sodium citrate, and 8.36 g of NaCl per litre of solution and pH was 3.0. The flow rate was 0.25 mL/min. The reactor temperature was set to 120°C. For dilution of samples, the diluting buffer was used (composition: Thiodiglycol 5 mL/L, citric acid 14 g/L, sodium chloride 11.5 g/mL).

2.8 ESI quadrupole TOF MS

ESI-Q-TOF-MS was another method for sarcosine analysis after establishing of bond between sarcosine and PMPs. For sarcosine determination Bruker Maxis Impact Q-TOF mass spectrometer (Bruker, Germany) was used. The ESI source was operated in a positive mode. The voltage of the electrospray capillary was set to 3 500 V with nebulizing gas (N_2) flow rate of 4 L/min and drying gas temperature set to 350°C. The flow of the injected sample was 180 μL/h. Scanning was carried out within the range from 50 to 1000 m/z. The sample was diluted in isopropanol a thousand times prior analysis.

2.9 HPLC with ED

For the determination of sarcosine, a system consisting of three chromatographic pumps Model 582 ESA (ESA, Chelmsford, MA, USA; working range 0.001–9.999 mL/min) was used. Two pumps was used for separation mobile phase A (ACN) and B (deionized Mili-Q water) to the column and third pump was connected behind the column just before the detector for the postcolumn addition of mobile phase C (phosphate buffer) for effective ED. For separation the HILIC chromatographic column Luna HILIC 200A (150 × 4.6; 3.5 μm particles, Phenomenex, Torrance, CA, USA) was used. The column was thermostatted at room temperature. As electrochemical detector four-channel CoulArray electrochemical detector (Model 5600A, ESA, Chelmsford, MA, USA) was used. The detector consists of one flow analytical chamber (Model 6210, ESA, Chelmsford, MA, USA), which contains four analytical cells. One analytical cell contains two reference electrodes (hydrogen-palladium), two counter electrodes and one porous graphite working electrode. The electrochemical detector was situated in control module, which was thermostatted. The sample (5 μL) was injected manually by an injection valve (Rheodyne, Oak Harbor, WA, USA) and injection needle (Hamilton, Reno, NV, USA).

2.10 Descriptive statistics

Mathematical analysis of these data and their graphical interpretation were realized by Microsoft Excel®, Microsoft Word® and Microsoft PowerPoint®. The results are expressed as mean ± SD unless noted otherwise. The detection limits (3 S/N) were calculated according to Long and Winefordner [28], whereas N was expressed as the standard deviation of noise determined in the signal domain unless stated otherwise.

2.11 Accuracy, precision, and recovery

The accuracy, precision, and recovery of sarcosine were evaluated with artificial urine spiked with a standard. Before extraction, 100 μL sarcosine and 100 μL water were added to artificial urine. Homogenates were assayed blindly and sarcosine concentration was derived from the calibration curve. The spiking of sarcosine was determined as a standard measured without the presence of a real sample. The accuracy was evaluated by comparing estimated concentrations with known concentrations of sarcosine. Calculation of accuracy (Bias, %), precision (CV, %), and recovery were carried out as indicated by Causon [29] and Bugianesi et al. [30].

3 Results and discussion

HPLC is one of the most widely utilized techniques for the determination of amino acids [31]. The post- or precolumn derivatization used to enhance UV detection sensitivity and/or to provide possibility of the chromatographic separation using a reversed phase is a disadvantage complicating amino acids analysis [32]. It is because the free amino acids are not, due to their polarity, retained in RP columns. The possibility of amino acids separation without derivatization steps is provided only by columns imitating the HILIC conditions [3, 33, 34]. Frequently applied detection with MS is able to resolve differences in retention times in seconds because of the possibility to set detection parameters [34]. Contrary to this the conventional detectors such as UV, DAD, or ED need better separation resolution, but on the other hand it can serve as cheaper alternative to expensive MS such as Orbitrap [34], triple-quadrupole [3], or ESI-TOF [35] commonly used for urine analyses. Next to this fact, there remains the immeasurable advantage of possible detector miniaturization, offering the option of detection by self-standing sensors based on paramagnetic particles as it is also shown below in this study.

3.1 HPLC–ED system

At a high applied potential, sarcosine easily undergoes oxidation, providing a signal to the detector. It is a very convenient characteristic for ED whose advantage is higher selectivity and sensitivity compared with UV detectors as it clearly follows from previously published results where the LOD for sarcosine obtained using the same detector in the flow injection analysis mode was estimated as 110 nM [14]. Sarcosine is an amino acid with characteristics improper for separation using RP columns; nevertheless it has presumptions for the separation on HILIC columns. The disadvantage of HILIC columns for sarcosine separation with consequent ED is the incompatibility of the elution of mobile phases with EDs, due to their polarities, which alter the detection limit [36–38]. In this study, we designed a system that consisted of a classical binary gradient using two chromatographic pumps, transporting the mobile phases to HILIC column and thus enable sarcosine separation and the third chromatographic pump connected into system behind the column served for the addition of the detection buffer allowing ED (Fig. 1). The sarcosine was thus delivered to the detector in the presence of an electrolyte, which is necessary for ED by coulometric detection (Fig. 1). The ratio of the mobile phase eluting from column to the postcolumn mixed electrolyte was 1:1. This setup effectively solved the issue with incompatibility of the elution mobile phases and ED. In this manner, the overall charge required for oxidation of total sarcosine amount during its flow through porous graphite working electrode was recorded. As a result, a high sensitivity for sarcosine analysis was achieved. Analysis in this way may be used for the determination of other amino acids such as glutamine involved

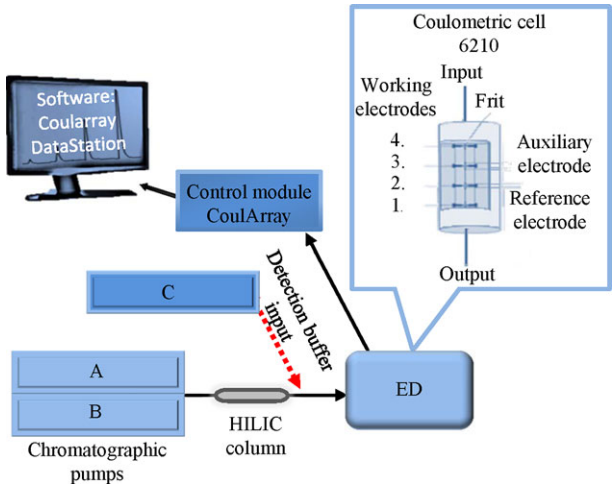

Figure 1. Scheme of the chromatographic system with an HILIC stationary phase and electrochemical detector. A and B mobile phases carry out the separation and C mobile phase contains the detection buffer. As electrochemical detector the four channel coulometric cell was used.

in metabolic pathways important in the occurrence of other malignancies [39–41].

3.2 Characterization of PMPs

Before we employed the HILIC–ED system for sarcosine analysis in real samples, we decided to use the paramagnetic particles (prepared according to Section 2.2 for the magnetic preseparation of sarcosine from the sample. For that purpose, the characterization of such particles was needed. We performed analysis by SEM as a first step of the characterization of our PMPs (Fig. 2A and B). SEM is an efficient way to characterize the surface morphology of different materials including PMPs [42]. The surface of $Gd(ClO_4)_3$ is covered by crystals of nanomaghemite that form a modern advanced material used in various fields of scientific, technological, and biomedical sectors [43, 44]. It clearly follows from the results obtained that nanomaghemite covers the majority of a PMP surface and thus provides perfect paramagnetic attributes very important in the workflow process. Furthermore, we carried out analysis on a scanning electrochemical microscope (SECM) to observe the changes of PMPs surface relative current response in the presence of sarcosine. An expression of the relative current response of PMP surface without sarcosine bound as a 3D image is shown in Fig. 2C. When compared with Fig. 2D, considerable changes of surface current response can be observed. Its current value is higher than before sarcosine binding. This obvious difference indicates that sarcosine binding leads to a change of PMPs attributes. Acidic Britton–Robinson buffer residues (pH 2) used during workflow process cause sarcosine protonation leading to a positive charging of sarcosine molecules with pI 6.2 [27]. Based on these results, we can conclude that we received a confirmation that PMPs bind sarcosine

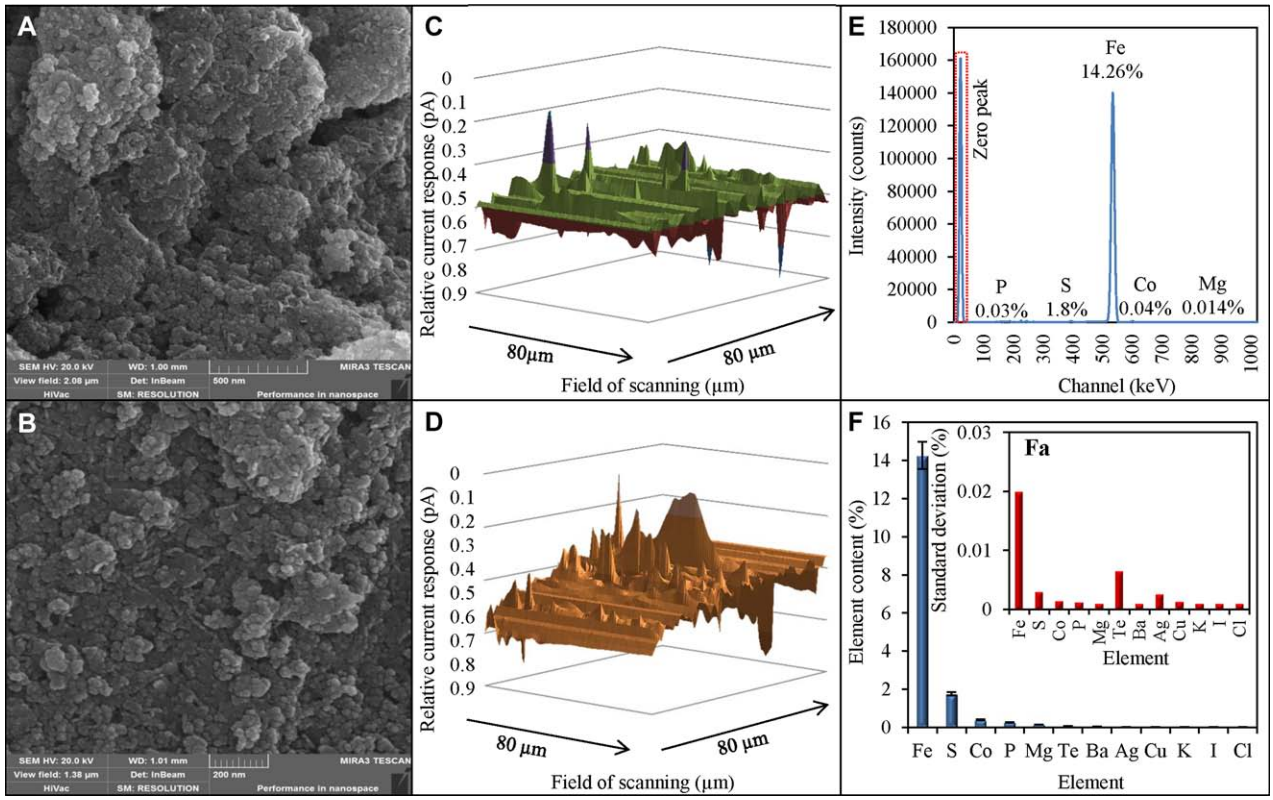

Figure 2. Characterization of PMPs. (A) SEM characterization of PMPs surface with magnified to 500 nm, (B) more detailed scan of PMPs zoomed to 200 nm. Both scans were obtained using a MIRA3 LMU SEM with a Schottky field emitter. (C) SECM 3D imaging characterization of PMPs surface without sarcosine bound, (D) SECM 3D imaging characterization of PMPs surface with sarcosine bound. Scans were obtained on scanning electrochemical microscope. (E) X-ray elemental analysis of PMPs, and (F) elemental representation contained in PMPs with (Fa) as an expression of SDs of measurements for each element.

properly and are usable for subsequent experiments. Additionally, we performed an elemental analysis of PMPs revealing the most represented elements forming our particles (Fig. 2E). As the most abundant element, Fe (14.26% of the total content) was determined. That fact was not surprising due to the manufacturing process of the particles crafting. Other elements present judging by their contents were S (1.8%), Co (0.04%), P (0.03%), and Mg (0.014%). Determined were also other elements such as Te, Ba, Ag, Cu, K, I, or Cl, but in ultra-trace amounts (Fig. 2F). SDs of measurements are shown in Fig. 2Fa. Elemental composition affects the specificity and other binding attributes of PMPs, thus elemental characterization of microparticles may show very important information about their behavior.

3.3 Analysis of sarcosine bound to PMPs

Prior to instrumental analysis, there is often a requirement for the isolation and preconcentration of the analyte. Urine is one of the most accessible body fluids for metabolomics applications [45], nevertheless, urine volume and composition vary widely [46]. Urine still acts as biological matrix containing interferents able to reduce the effectiveness of analytical assays, thus a preconcentration of sarcosine may play crucial role in the analysis of real sample. We carried out the preconcentration of sarcosine using modified PMPs (Fig. 3). The surface of PMPs was modified by maghemite (γ-Fe_2O_3) nanoparticles, which are gaining great interest in analytical chemistry for their small size and high surface area providing better kinetics as well as the possibility of manipulation under the influence of an external magnetic field [47–50]. The isolation process can be performed directly in samples containing the analyte, which eliminates the need for centrifugation or filtration [51]. We coated maghemite nanoparticles with tris(perchlorate)gadolinium and surprisingly the particles showed the appropriate properties for sarcosine binding (Table 1). Interday precision was evaluated by determining five replicates over three consecutive days ($n = 15$) with recoveries within the range from 31 to 42% and RSD of <5.32% in intraday analysis and <6.39% for interday analysis. Utilization of PMPs provides a relatively quick, simple, effective, and suitable preconcentration approach. We performed analyses on IEC and MS for the confirmation of the presence of sarcosine and comparison of analysis accuracy. IEC results showed very similar recoveries of sarcosine from PMPs (Fig. 4A), particularly 35% with retention time approximately at 18 min. That was a confirmation for us that PMPs are

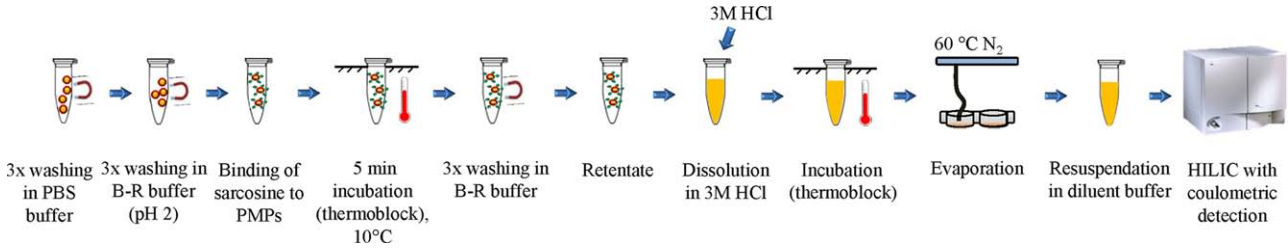

Figure 3. Workflow scheme of sarcosine isolation with PMPs.

applicable for sarcosine binding and may be used for subsequent HILIC–ED experiments. Mass spectra of sarcosine confirm the presence of the analyte after the whole workflow process (Fig. 4B).

3.4 Optimization of sarcosine separation

The objective of optimizing the separation was to obtain the lowest retention time for sarcosine as possible with preserving of the good resolution of separation. For sarcosine retention, ACN as a mobile phase A and MiliQ water as a mobile phase B were utilized. For the separation of sarcosine (500 μg/mL), we used a total flow rate of 1 mL/min (0.5 mL/min from column and 0.5 mL/min from the third "buffer" pump) and detector potential of 1000 mV. The evaluation of the ACN concentration effect on the separation efficiency was performed as a calculation of a number of theoretical plates $5.54 \times (t_r/Y_{0.5})^2$, where t_r is a retention time and $Y_{0.5}$ peak width in its half, indicating the chromatographic column separation efficiency. The larger it is, the less is the broadened zone of separated substance passing through the column and the peak is narrower in the chromatogram and has the higher time distance from the dead volume in the

Table 1. Intra- and interday precision and accuracy of PMPs used for sarcosine preconcentration

Compound	Concentration ($\mu g.mL^{-1}$)	Intraday ($n = 6$) CV (%)	Recovery (%)	Interday ($n = 15$) CV (%)	Recovery (%)
Sarcosine	12.5	4.29	31	6.26	31
	25	5.01	35	5.88	32
	50	4.88	36	6.39	37
	100	3.39	41	6.03	38
	200	5.32	43	5.38	42

CV: coefficient of variation.

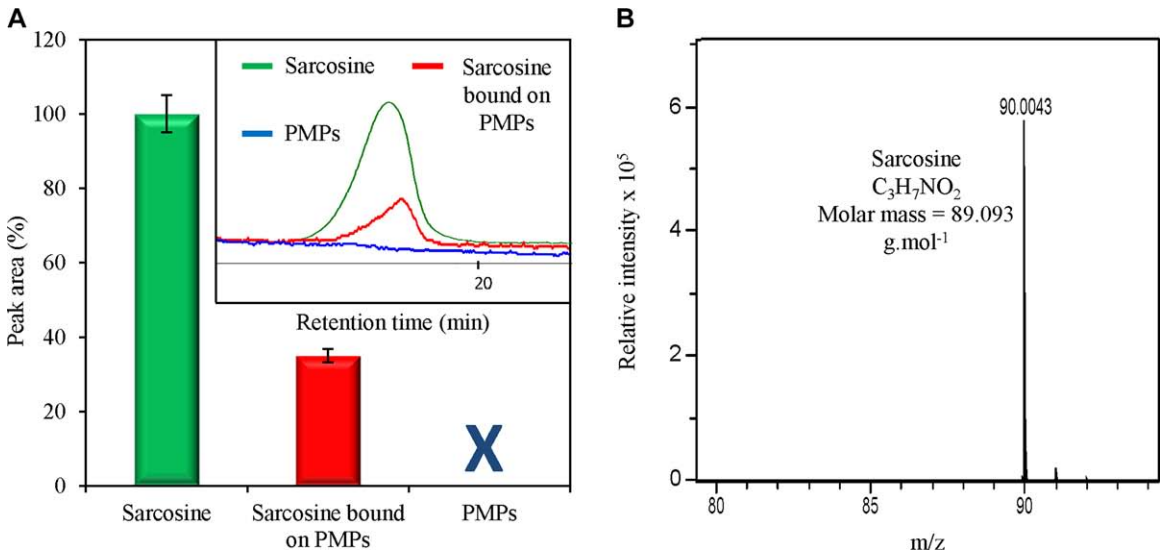

Figure 4. (A) IEC analysis of sarcosine after establishing binding between PMPs and sarcosine (100 μg/mL). (B) ESI-Q-TOF-MS signal of sarcosine diluted in isopropanol after binding on PMPs surface.

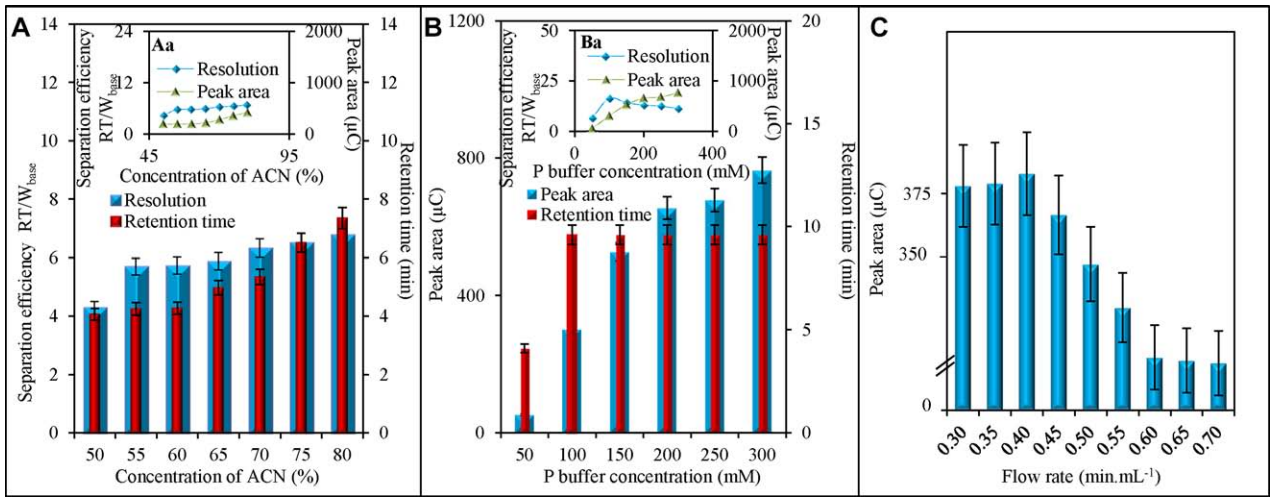

Figure 5. Optimization of sarcosine HILIC separation and detection. (A) Representation of the influence of ACN concentration (50, 55, 60, 65, 70, 75, and 80%, v/v) on the separation of sarcosine (500 μg/mL). (Aa) The expression of dependence of the resolution of sarcosine (500 μg/mL) on peak area. (B) The influence of P (phosphate) buffer concentration (50, 100, 150, 200, 250, and 300 mM) on the resolution of sarcosine (500 μg/mL). (Ba) The expression of dependence of resolution of sarcosine (500 μg/mL) on its peak area. (C) The influence of flow rate of mobile phases on sarcosine (500 μg/mL) detection.

same time. It follows from the results obtained (Fig. 5A) that efficiency of column was increasing from 50 to 70% of ACN. At 70% we observed maximum, where peak broadening is not significant and number of theoretical plates is the largest. Subsequently, we observed a decrease of column efficiency at higher tested ACN concentrations (from 80–90%). With the increasing addition of ACN we observed the increasing retention time. In Fig. 5Aa, we show the relationship between the resolution of sarcosine detected and its peak area for each tested concentration of ACN. For HILIC separation it is also common to utilize an aqueous phase with salt addition (buffers) to enhance ion exchange actions during separation and thus to improve the resolution. Despite this fact from our preliminary analyses we did not find any improvement of the separation when acetic buffer with pH 5 or ammonium acetate with pH 5 (both in 100 mM concentration) was used as aqueous part of the mobile phase. Additionally, the slightly negative effect on the sensitivity of the detection caused by decreasing the overall pH of the "detection" phosphate buffer was reported. Therefore, we used only water as the aqueous part of the mobile phase for separation.

3.5 Optimization of sarcosine detection

Although HILIC works on opposite interactions between the stationary and mobile phases and separation is influenced by nonpolar reagents, lowering the electrochemical response, it was necessary to connect the postcolumn addition of detection buffer, allowing the sarcosine ED. Therefore during the optimization of sarcosine detection ratio of postcolumn addition of buffer was also of our interest. On the basis of previous experiments [27], phosphate buffer with pH 9 (P buffer) was chosen and showed the best properties for the sarcosine detection. An optimization of phosphate buffer concentration (50, 100, 150, 200, 250 and 300 mM) was also necessary (Fig. 5B). It clearly follows from the results obtained that concentration of 200 mM was sufficient for sarcosine detection under conditions maintained by our three mobile phases. At higher concentrations of phosphate buffer slightly higher peak areas were observed, but there were also issues with precipitation of phosphate buffer before the detector followed by the increasing backpressure on the detector (only when >200 mM was used). In Fig. 5Ba, there are obvious very similar trends of resolution and peak area of different concentrations of phosphate buffer. The detector response was roughly tested with ratio of column output containing the analyte and ACN and "detection" P buffer output (1:1). This ratio was found as an ideal compromise between logical drawbacks, which appeared when we attempted to change it: (i) when the flow rate in the column output is increased the sarcosine concentration is higher when coming to the detector but the ACN concentration is higher as well, which both decreased the concentration of "detection buffer" coming from the P buffer output, which results overall decrease of sensitivity, (ii) when the ratio setting is turned opposite to the concentration of sarcosine, output from the column is decreased the same as the ACN but even the resolution of separation is decreased because of higher dilution factor making peak of sarcosine wider and lower and the fact that the concentration of P buffer is increased does not help enough to enhance the sensitivity.

After the optimization of the above-mentioned conditions, we tested the influence of the total flow rate. Sarcosine (500 μg/mL) was analyzed at flow rates 0.30, 0.35, 0.40, 0.45, 0.50, 0.55, 0.60, 0.65, and 0.7 mL/min. At a higher flow rate, we observed a decrease of the electrochemical signal and electrochemical detector. It clearly follows from the results obtained that the increase of the

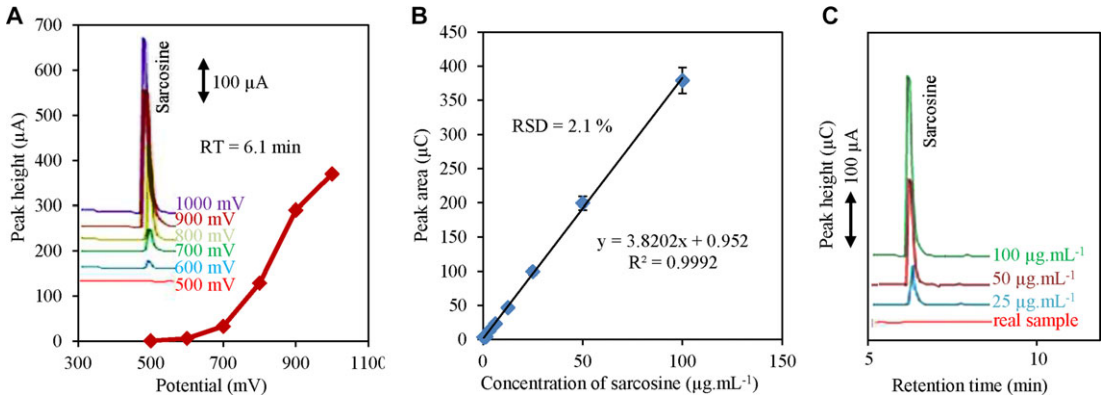

Figure 6. Optimization of sarcosine detection. (A) The influence of potential on the peak area of sarcosine (100 μg/mL) with a flow rate of 0.40 mL/min. (B) Calibration curve of sarcosine measured within the range from 0.3 to 100 μg/mL carried out under conditions optimized in previous analysis at a flow rate 0.40 mL/min and potential of 1000 mV. (C) Array records of different concentrations (12.5, 50, and 100 μg/mL) of sarcosine obtained using PMPs after HILIC separation compared to the array record of a urine sample obtained from a healthy individual.

peak area between 0.30 and 0.40 mL/min and subsequent downward trend until 0.7 mL/min was observed (Fig. 5C). A signal of more commonly used amperometric detection closely relates to a flow rate of mobile phase but by the coulometric detectors, which are used herein, and the situation should not be so critical. Because of the much higher efficiency of electron transfer, which is given by the much higher surface area of the working electrode in a coulometric detector, the flow rate might not influence the peak area so much. It is because the difference of yield of the analyte's redox change is >85% between the amperometric and coulometric detector [52]. Over that, the peak area decreases with higher flow rate. This phenomenon was probably caused by saturation of the active electrode surface [36]. Our results confirmed the reduction of the coulometric detector response, when the maximum response was obtained at a flow rate on the column output of 0.40 mL/min. When both outputs were at a ratio of 1:1 there was a total flow rate of 0.80 mL/min on the coulometric cell, which corresponds to our previously obtained data [52].

To determine the maximum oxidation potential of sarcosine, the hydrodynamic voltammograms were determined indicating the dependence of the peak area on inputting voltage (500–1000 mV). From the obtained voltammograms (Fig. 6A) it is obvious that the peak area was increased to 1000 mV, where it was reported the oxidation maximum of sarcosine.

3.6 Method validation

The method for the determination of sarcosine by HILIC with ED was validated by analysis of sarcosine standards. Standard solution of sarcosine (100 μg/mL, 10 μL) was injected and following optimal conditions were determined: mobile phase A ACN, mobile phase B water in ratio A/B 70:30, and postcolumn addition of mobile phase C (200 mM phosphate buffer pH 9). The optimal mixing ratio was A + B/C 1:1 with a flow rate of 0.80 mL/min (0.40 + 0.40 mL/min as it was optimized). We also carried out the analyses of peak asymmetries to indicate the possibility of column overloading, the stationary phase surface heterogeneity, the heterogeneity of the column packing, and the extra-column effects [53, 54].

In separation optimization steps we used a flow rate of 1 mL/min corresponding with our preliminary results and we obtained the asymmetry of 1.198. The asymmetry at the ideal flow rate for detection (0.4 mL/min) was established as 1.311. Both asymmetries showed similar numbers. Because we used PMPs for preconcentration, perfect separation of sarcosine was not our primary goal in contrast to optimal conditions for its detection. For this purpose the electrochemical potential was set to 1000 mV (Fig. 6A), and under these optimal conditions calibration curve was measured (Fig. 6B). The LOD (3 S/N) was estimated as 100 nM, and the results are summarized in Table 2 as well as other parameters of analysis. We also carried out intra- and interday precision data estimation (Table 3). Interday precision was evaluated by determining five replicates over three consecutive days ($n = 15$). The results showed good average of relative recoveries within the range from 98 to 99% with good RSD of <4.97% in intraday analysis and <5.31% for interday analysis. When compared to other methods used for sarcosine separation and detection, such as LC–MS, used by Meyer et al. with LOD of 5 nM [3], HPLC–MS/MS used by Jiang et al. with an LOD of 3 nM [15]. Using a method of derivatization with liquid–liquid microextraction in combination with LC–MS as well as GC–MS, Shamsipur et al. reached a LOD of 1 nM [55]. Although commonly used MS analysis shows better LODs, there is the advantage of possible electrochemical detector miniaturization, offering the option of detection via self-standing sensors based on paramagnetic particles.

3.7 Artificial urine analysis

Artificial urine was made according to ref. [56] and spiked with 100 μg/mL of sarcosine as an internal standard in volume of

Table 2. Analytical parameters of HILIC-ED detection of sarcosine

Compound	Retention time (min)	Linear regression Equation	Linear dynamic range (μM)	Linear dynamic range (μg/mL)	R^2[a]	LOD[b] (nM)	LOD (ng/mL)	LOD (fmol) per injection	LOQ[c] (nM)	LOQ (ng/mL)	LOQ (fmol)[d] per injection	RSD[e] (%)
Sarcosine	6.1	$y = 3.8202x + 0.952$	0.07–561	0.024–50	0.9992	100	10	1.1	380	34	3.8	2.1

a) Regression coefficient.
b) Limit of detection (3 S/N).
c) Limit of quantification (10 S/N).
d) Injection of 5 L volume.
e) Relative standard deviation.

Table 3. Intra- and interday precision and accuracy of HILIC-ED

Compound	Concentration (μg/mL)	Intraday ($n = 8$) CV (%)	Recovery (%)	Interday ($n = 15$) CV (%)	Recovery (%)
Sarcosine	25	3.97	99	4.31	98
	50	3.93	99	3.29	97
	100	2.22	97	3.27	95

CV, coefficient of variation.

100 μL in ratio 1:1 with water added to artificial urine samples. Sarcosine recoveries were evaluated in artificial urine spiked with standard of sarcosine with preconcentration step using PMPs. Samples were assayed blindly and sarcosine concentrations were derived from the calibration curve. The spiking of sarcosine was determined as an internal standard measured without presence of real sample. It clearly follows from the chromatograms obtained that no change occurred in the retention time (Fig. 6C). Good results were obtained according to relatively good recovery in intra- (82%) and interday (80%) analysis. The LOD in artificial urine was established at 130 nM (Table 4). This can serve as a confirmation that PMPs connected with HILIC–ED analysis may be used as a novel analytical method for determination of sarcosine low levels in urine. Troublesome are apparently interferents commonly contained in urine lowering by their properties binding of sarcosine on paramagnetic particles surface [27], and thus decrease sarcosine recovery (25%).

Table 4. Analytical parameters of HPLC-ED detection of sarcosine standard (100 μg/mL) in artificial urine

Compound	Sarcosine	
Retention time	(min)	6.8
Linear regression	Equation	$y = 0.8498x + 1.1384$
Linear dynamic range	(μg/mL)	0.04–75
R^2[a]		0.989
LOD[b]	(nM)	130
LOD	(ng/mL)	13
LOD (fmol)	per injection	1.2
LOQ[c]	(nM)	420
LOQ	(ng/mL)	43
LOQ (fmol)[d]	per injection	4.2
RSD[e]	(%)	3.3
Intraday ($n = 4$)	CV (%)	4.66
Recovery	(%)	26
Interday ($n = 9$)	CV (%)	5.23
Recovery	(%)	25

a) Regression coefficient.
b) Limit of detection (3 S/N).
c) Limit of quantification (10 S/N).
d) Injection of 5 L volume.
e) Relative standard deviation.

4 Concluding remarks

A method for sarcosine determination using HPLC with a HILIC stationary phase and ED was developed. This novel method has several advantages such as a relatively cheap acquisition price when comparing with mass spectrometers commonly used for urine analysis and very low LOD sufficient for analysis of samples of patients suffering from prostate cancer. In addition we connected an approach using PMPs for the preconcentration of the analyte in a sample. These approaches together may serve as a novel method for low-level sarcosine detection in the diagnosis of prostate cancer, which has an LOQ 420 nM below the commercially available photometric kits. Our Approach using PMPs also shows a potential to serve as a tool for the immobilization of sarcosine molecules in a lab-on-a-chip device. As was shown by Llopis et al., the utilization of paramagnetic particles in lab-on-a-chip approach enables the easy renewal of the biosensing material after determination in a highly reproducible manner [57]. Biosensors crafted in this way may improve the detection of prostate carcinoma, and thus ensure the early diagnostics of disease, leading to improved prognoses.

Financial support from CYTORES GA CR P301/10/0356 and CEITEC CZ.1.05/1.1.00/02.0068 is gratefully acknowledged. Special thanks are dedicated to TESCAN, a.s., Brno for

acquiring the paramagnetic microparticles images on a scanning electron microscope.

The authors have declared no conflict of interest.

5 References

[1] Mitchell, A. D., Benevenga, N. J., *J. Nutr.* 1976, *106*, 1702–1713.

[2] Sreekumar, A., Poisson, L. M., Rajendiran, T. M., Khan, A. P., Cao, Q., Yu, J. D., Laxman, B., Mehra, R., Lonigro, R. J., Li, Y., Nyati, M. K., Ahsan, A., Kalyana-Sundaram, S., Han, B., Cao, X. H., Byun, J., Omenn, G. S., Ghosh, D., Pennathur, S., Alexander, D. C., Berger, A., Shuster, J. R., Wei, J. T., Varambally, S., Beecher, C., Chinnaiyan, A. M., *Nature* 2009, *457*, 910–914.

[3] Meyer, T. E., Fox, S. D., Issaq, H. J., Xu, X., Chu, L. W., Veenstra, T. D., Hsing, A. W., *Anal. Chem.* 2011, *83*, 5735–5740.

[4] Struys, E. A., Heijboer, A. C., van Moorselaar, J., Jakobs, C., Blankenstein, M. A., *Ann. Clin. Biochem.* 2010, *47*, 282–282.

[5] Cao, D. L., Ye, D. W., Zhu, Y., Zhang, H. L., Wang, Y. X., Yao, X. D., *Prostate Cancer Prostatic Dis.* 2011, *14*, 166–172.

[6] Jentzmik, F., Stephan, C., Miller, K., Schrader, M., Erbersdobler, A., Kristiansen, G., Lein, M., Jung, K., *Eur. Urol.* 2010, *58*, 12–18.

[7] Schalken, J. A., *Eur. Urol.* 2010, *58*, 19–20.

[8] Burton, C., Gamagedara, S., Ma, Y. F., *Anal. Methods* 2012, *4*, 141–146.

[9] LeBoucher, J., Charret, C., CoudrayLucas, C., Giboudeau, J., Cynober, L., *Clin. Chem.* 1997, *43*, 1421–1428.

[10] Sherwood, R. A., Titheradge, A. C., Richards, D. A., *J. Chromatogr. Biomed. Appl.* 1990, *528*, 293–303.

[11] Yi, P., Liu, L., Mei, H. F., Zeng, F. L., Huang, Z. J., Niu, H. L., *J. Pediatr. Endocrinol. Metab.* 2011, *24*, 733–738.

[12] Cavaliere, B., Macchione, B., Monteleone, M., Naccarato, A., Sindona, G., Tagarelli, A., *Anal. Bioanal. Chem.* 2011, *400*, 2903–2912.

[13] Bianchi, F., Dugheri, S., Musci, M., Bonacchi, A., Salvadori, E., Arcangeli, G., Cupelli, V., Lanciotti, M., Masieri, L., Serni, S., Carini, M., Careri, M., Mangia, A., *Anal. Chim. Acta* 2011, *707*, 197–203.

[14] Cernei, N., Zitka, O., Ryvolova, M., Adam, V., Masarik, M., Hubalek, J., Kizek, R., *Int. J. Electrochem. Sci.* 2012, *7*, 4286–4301.

[15] Jiang, Y. Q., Cheng, X. L., Wang, C. A., Ma, Y. F., *Anal. Chem.* 2010, *82*, 9022–9027.

[16] Martinez-Lozano, P., Rus, J., *J. Am. Soc. Mass Spectrom.* 2010, *21*, 1129–1132.

[17] Cernei, N., Zitka, O., Skalickova, S., Gumulec, J., Sztalmachova, M., Rodrigo, M. A. M., Sochor, J., Masarik, M., Adam, V., Hubalek, J., Trnkova, L., Kruseova, J., Eckschlager, T., Kizek, R., *Oncol. Rep.* 2013, *29*, 2459–2466.

[18] Alpert, A. J., *J. Chromatogr.* 1990, *499*, 177–196.

[19] Guo, H. Y., Liu, R. H., Yang, J. J., Yang, B. C., Liang, X. M., Chu, C. H., *J. Chromatogr. A* 2012, *1223*, 47–52.

[20] Ikegami, T., Tomomatsu, K., Takubo, H., Horie, K., Tanaka, N., *J. Chromatogr. A* 2008, *1184*, 474–503.

[21] Mora, L., Hernandez-Cazares, A. S., Aristoy, M. C., Toldra, F., Reig, M., *Food Anal. Methods* 2011, *4*, 121–129.

[22] Appelblad, P., Abrahamsson, P., *LC GC N. Am.* 2005, *2005*, 24–25.

[23] Ihunegbo, F. N., Tesfalidet, S., Jiang, W., *J. Sep. Sci.* 2010, *33*, 988–995.

[24] Jiang, W., Ihunegbo, F. N., *LC GC Eur.* 2009, *2009*, 21–23.

[25] Gratacos-Cubarsi, M., Sarraga, C., Clariana, M., Regueiro, J. A. G., Castellari, M., *Meat Sci.* 2011, *87*, 234–238.

[26] Nezirevic, D., Arstrand, K., Kagedal, B., *J. Chromatogr. A* 2007, *1163*, 70–79.

[27] Zitka, O., Cernei, N., Heger, Z., Matousek, M., Kopel, P., Kynicky, J., Masarik, M., Kizek, R., Adam, V., *Electrophoresis* 2013, *34*, 2639–2647.

[28] Long, G. L., Winefordner, J. D., *Anal. Chem.* 1983, *55*, 712A-724A.

[29] Causon, R., *J. Chromatogr. B* 1997, *689*, 175–180.

[30] Bugianesi, R., Serafini, M., Simone, F., Wu, D. Y., Meydani, S., Ferro-Luzzi, A., Azzini, E., Maiani, G., *Anal. Biochem.* 2000, *284*, 296–300.

[31] Pereira, V., Pontes, M., Camara, J. S., Marques, J. C., *J. Chromatogr. A* 2008, *1189*, 435–443.

[32] Frank, M. P., Powers, R. W., *J. Chromatogr. B* 2007, *852*, 646–649.

[33] Kuban, P., Hauser, P. C., *J. Chromatogr. A* 2006, *1128*, 97–104.

[34] Gokmen, V., Serpen, A., Mogol, B. A., *Anal. Bioanal. Chem.* 2012, *403*, 2915–2922.

[35] Armstrong, M., Jonscher, K., Reisdorph, N. A., *Rapid Commun. Mass Spectrom.* 2007, *21*, 2717–2726.

[36] Petrlova, J., Mikelova, R., Stejskal, K., Kleckerova, A., Zitka, O., Petrek, J., Havel, L., Zehnalek, J., Adam, V., Trnkova, L., Kizek, R., *J. Sep. Sci.* 2006, *29*, 1166–1173.

[37] Potesil, D., Petrlova, J., Adam, V., Vacek, J., Klejdus, B., Zehnalek, J., Trnkova, L., Havel, L., Kizek, R., *J. Chromatogr. A* 2005, *1084*, 134–144.

[38] Klejdus, B., Mikelova, R., Petrlova, J., Potesil, D., Adam, V., Stiborova, M., Hodek, P., Vacek, J., Kizek, R., Kuban, V., *J. Chromatogr. A* 2005, *1084*, 71–79.

[39] Shaw, R. J., Cantley, L. C., *Nature* 2006, *441*, 424–430.

[40] Commisso, C., Davidson, S. M., Soydaner-Azeloglu, R. G., Parker, S. J., Kamphorst, J. J., Hackett, S., Grabocka, E., Nofal, M., Drebin, J. A., Thompson, C. B., Rabinowitz, J. D., Metallo, C. M., Vander Heiden, M. G., Bar-Sagi, D., *Nature* 2013, *497*, 633–637.

[41] Son, J., Lyssiotis, C. A., Ying, H., Wang, X., Hua, S., Ligorio, M., Perera, R. M., Ferrone, C. R., Mullarky, E., Ng, S. C., Kang, Y., Fleming, J. B., Bardeesy, N., Asara, J. M., Haigis, M. C., DePinho, R. A., Cantley, L. C., Kimmelman, A. C., *Nature* 2013, *496*, 101–105.

[42] Zhang, X., Chen, P., Yu, Q., Ma, K., Ding, Z., Zhu, X., *Vacuum* 2013, *97*, 1–8.

[43] Tucek, J., Zboril, R., Petridis, D., *J. Nanosci. Nanotechnol.* 2006, *6*, 926–947.

[44] Magro, M., Sinigaglia, G., Nodari, L., Tucek, J., Polakova, K., Marusak, Z., Cardillo, S., Salviulo, G., Russo, U., Stevanato, R., Zboril, R., Vianello, F., *Acta Biomater.* 2012, *8*, 2068–2076.

[45] Ryan, D., Robards, K., Prenzler, P. D., Kendall, M., *Anal. Chim. Acta* 2011, *684*, 17–29.

[46] Mattarucchi, E., Guillou, C., *Biomed. Chromatogr.* 2012, *26*, 512–517.

[47] Giakisikli, G., Anthemidis, A. N., *Talanta* 2013, *110*, 229–235.

[48] Zong, P. F., Wang, S. F., Zhao, Y. L., Wang, H., Pan, H., He, C. H., *Chem. Eng. J.* 2013, *220*, 45–52.

[49] Rittich, B., Spanova, A., *J. Sep. Sci.* 2013, *36*, 2472–2485.

[50] Huang, X. J., Wang, Y. L., Liu, Y., Yuan, D. X., *J. Sep. Sci.* 2013, *36*, 3210–3219.

[51] Karamani, A. A., Douvalis, A. P., Stalikas, C. D., *J. Chromatogr. A* 2013, *1271*, 1–9.

[52] Sochor, J., Dobes, J., Krystofova, O., Ruttkay-Nedecky, B., Babula, P., Pohanka, M., Jurikova, T., Zitka, O., Adam, V., Klejdus, B., Kizek, R., *Int. J. Electrochem. Sci.* 2013, *8*, 8464–8489.

[53] Papai, Z., Pap, T. L., *J. Chromatogr. A* 2002, *953*, 31–38.

[54] Bosakova, Z., Curinova, E., Tesarova, E., *J. Chromatogr. A* 2005, *1088*, 94–103.

[55] Shamsipur, M., Naseri, M. T., Babri, M., *J. Pharm. Biomed. Anal.* 2013, *81-82*, 65–75.

[56] Brooks, T., Keevil, C. W., *Lett. Appl. Microbiol.* 1997, *24*, 203–206.

[57] Llopis, X., Pumera, M., Alegret, S., Merkoci, A., *Lab Chip* 2009, *9*, 213–218.

